PAPER

Collection of dim light for accurate optical polarimetry by a plano-convex spherical lens

IOP Publishing Measurement Science and Technology
Meas. Sci. Technol. **33** (2022) 015201 (8pp) https://doi.org/10.1088/1361-6501/ac2dba

Collection of dim light for accurate optical polarimetry by a plano-convex spherical lens

K D Foreman* **and T J Gay**

Jorgensen Hall, University of Nebraska, Lincoln, NE 68588-0299, United States of America

E-mail: keith.foreman@unl.edu

Received 2 September 2021
Accepted for publication 7 October 2021
Published 21 October 2021

Abstract

High-accuracy optical polarimetry of atomic fluorescence generally requires the use of a collimating collection lens. The orientation of this lens can affect its transmission due to reflective loss, but can also change the polarization state of the light being measured. Current best practices regarding lens orientation are related to minimizing spherical aberration. In this work, we use the ray-tracing software TracePro® to investigate the matter of lens orientation for a plano-convex lens as it relates to light transmission and reflection- and refraction-induced polarization changes. We compare the amount of scattered light for both orientations of the lens with and without anti-reflection coating, and show the effect the lens has on the polarization of the light produced by an unpolarized point-source as well as two point sources simulating highly-polarized atomic fluorescence. We discuss how these effects can be of concern for polarization-sensitive imaging and polarimetry of dim light sources with an accuracy of better than 0.1% of the measured Stokes parameters.

Keywords: polarimetry, refraction, reflection, collimating-lens

(Some figures may appear in color only in the online journal)

1. Introduction

Accurate optical polarimetry plays an important role in, for example, astronomical observations [1, 2], magneto-optical Kerr studies of magnetized surfaces [3, 4], and atomic parity violation experiments [5, 6]. Recently, it has been proposed that a calibration standard for highly precise Mott electron polarimetry could be based on measuring the fluorescence polarization of atoms excited by spin-polarized electrons to better than 0.1% of the Stokes parameters being measured (Accurate Electron Spin Optical Polarimetry—AESOP) [7–9]. Indeed, the precise measurement of atomic fluorescence polarization has served as an invaluable tool for the study of many aspects of electron–atom collisions [10, 11]. In these latter experiments, the light source of excited atoms is in a vacuum system, and the atomic fluorescence is collected by a lens, one focal length away from the source, after it passes through a vacuum window. This lens collimates the light before it passes through a suitable polarimetric optical train [12] and is focused onto the photocathode of a detector by a 2nd lens. Because these experiments generally involve dim sources, a photomultiplier tube coupled with photon-counting electronics is often used as the detector, and one tries to maximize the solid angle about the source subtended by the collection lens.

In the case of plano-convex collection lenses, a natural question that often occurs to the optical train designer is, should the flat side or the convex side face the source? One piece of folk wisdom regarding image formation says that ‘one should minimize the average angle of incidence of the light rays on the lens, which will reduce spherical aberration’. When doing an experiment that involves photon-limited-counting and/or high-accuracy polarimetry, however, questions regarding lens orientation arise unrelated to image formation. In the former case, where statistical accuracy is limited by the intensity of the source, the loss of reflected light becomes important.

* Author to whom any correspondence should be addressed.

The reflectivity of light generally decreases with decreasing angle of incidence, meaning that light loss due to reflectivity is minimized for the planar side of the lens facing upstream when collimating a point-source of light, and the opposite orientation when using the lens to refocus a collimated beam [13]. Light loss can also be reduced, of course, by coating the optical elements with anti-reflective (AR) coating, but here the orientation of the collection lens matters as well.

Very accurate polarimetry requires that changes in the polarization state of the light due to reflection and refraction at the collection lens surfaces be taken into account. Here, one might again think that the flat side of the collimation lens should face the source. This seems reasonable; Fresnel's equations tell us that the difference in reflectance and transmission for both the ordinary and extraordinary rays is minimized as the angle of incidence approaches zero.

These questions become increasingly important as the source intensity grows dimmer and/or polarimetric accuracy requirements become more stringent. To our knowledge, collection lens orientation and the effects of reflection and refraction on light transmission and polarization by a plano-convex lens, as they relate to photon counting and polarimetry experiments (as opposed to image formation) have not been addressed in the literature. In this paper, we present a quantitative analysis of these issues for application to the AESOP optical test polarimeter we have built at the University of Nebraska [7]. This device has a design accuracy goal of 0.1% of the polarization being measured. To do this, we simulate a point source/lens/polarimeter optical train using the proprietary software TracePro®. We consider a single, relatively large (2-inches diameter) plano-convex glass collection lens because of the general need, in a count-limited experiment, to maximize the light-gathering power of the system. Applicability of our findings to the requirements of very-high-accuracy optical polarimetry with dim light are discussed.

2. TracePro® simulations

The basic optical train used for these simulations, typical of the optical components used in an atomic fluorescence experiment, is shown in the left panel of figure 1. It consists of a point-source of light, a plano-convex collimating collection lens, a quarter-wave retarder (or 'analyzing retarder'), a linear polarizer ('analyzing polarizer'), and an opaque beam-stop used to collect the rays, and which effectively serves as the photodetector. The lenses in all simulations were one focal length away from the point-source, and all had a 2-inch diameter and 1.6-inch clear aperture (as does the AESOP optical polarimeter), defined by a geometric stop immediately upstream of the lens. Depending on which face of the lens was upstream, we adjusted the distance between the lens and the point source to optimize the parallelism of the rays transmitted by the lens. The designated focal length of the lens was determined by the 'lens-makers' equation [13]. The retarder and the polarizer were used to measure the polarization state of the light using the fast Fourier transform (FFT) analysis described in [12].

Unless noted, our simulations assumed that we were observing the Ne $3s^3P_2$–$3p^3D_3$ 640-nm transition, a standard used in optical electron polarimetry [8]. The simulated lens is made of N-BK7 glass and can be bare or AR coated with MgF_2. We assume that the reflected and transmitted rays of light obey Fresnel's equations [14] for an air/N-BK7 interface with or without AR coating. Special attention was given to the analyzing retarder in these simulations since it is this component that rotates about the transmission axis while the analyzing polarizer stays fixed during a polarization measurement [12]. Thus, when considering the Fresnel-induced polarization of the light transmitted through the lens, which will be manipulated further by the retarder, we must consider retarders that are not ideal, either because their fast axis has an ill-defined or spatially-variable angular orientation, or because the retardance varies across the clear aperture.

TracePro® can generate maps of the Stokes parameters of light incident upon a surface and can calculate the total transmitted intensity of the light through any particular optic. An opaque beam-stop was used to 'collect' the rays and generate these maps with a 0.508-mm resolution. Approximately 50 000 rays of light comprise the beam cross-sections.

Our simulations were conducted to provide feedback for the design and characterization of the AESOP high-accuracy optical test polarimeter, a photograph of which is shown in the right panel of figure 1. The point-source of the simulated optical train, discussed above, mimics polarized fluorescent light emitted by a small, well-defined atomic target. The simulated analyzing retarder, analyzing polarizer, and detection screen have physical counterparts shown as group 3 in the photo.

3. Results

3.1. Light scattering

In a count-rate limited experiment all photons are precious, so we initially consider how to minimize photon scattering due to reflection. Using first a simplified optical train comprising only a point-source, collection lens, and beam-stop, the percent of scattered light is measured for 2-inch diameter lenses with a range of focal lengths, both with and without an AR coating, and oriented with the planar and then the curved side upstream. Here, scattered light is defined as the missing fraction of power incident upon the lens that was not subsequently incident upon the beam-stop. Our simulations show that as the radius of curvature of an uncoated lens was increased from 35 mm to 300 mm, corresponding to a focal length range from 68 mm to 583 mm, the fraction of the incident scattered light varied from 8.9% to 8.3% with the curved surface of the lens facing upstream, and from 8.6% to 8.3% with the planar surface upstream. This variation is simply due to the fact that lenses with shorter focal lengths are struck by light beams with larger average angles of incidence, which are more efficiently reflected. Unsurprisingly, the situation is significantly improved when the lens is AR coated with total incident light scattering varying between 3.7% for the shortest focal lengths and 2.9% for the longest ones. Consistent with conventional

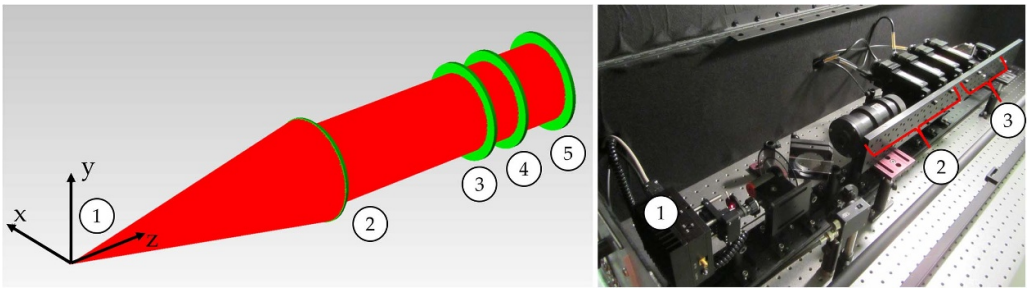

Figure 1. The simulated optical train (left), with the light rays shown in red and optical components in green including: (1) the point-source, (2) collimating collection lens, (3) analyzing retarder, (4) analyzing polarizer, and (5) opaque beam stop/detection screen. Photo of the AESOP high-accuracy test polarimeter (right) showing: (1) 640-nm diode laser, (2) beam expander and polarization-defining optics, and (3) polarimeter. Label (3) in the photo corresponds to simulated elements (3) through (5) in the left panel.

wisdom, the AR-coated lens oriented with the planar side upstream (toward the point-source) scatters the least amount of light, although this effect is not large.

3.2. *Fresnel-induced polarization*

We now address an issue of more importance for high-accuracy polarimetry that is the main focus of this paper: Fresnel-induced changes to the polarization state of the light transmitted by the collimating lens. For a point-source producing unpolarized light, figure 2 shows the typical linear Stokes polarization parameters, P_1 and P_2, of the beam in cross-section for the collimated light immediately after passing through the lens. The direction of propagation is into the page. The lens used in this simulation was AR coated, oriented with the planar side upstream, and had a focal length of 155 mm, though the data in figure 2 is generally representative of unpolarized light passing through any collimating lens.

Figure 2 shows that the light is no longer unpolarized after passing through the lens; a small contaminant polarization is now present. The Stokes polarization parameter P_1 characterizes the linear polarization fraction referenced along the horizontal and vertical (x- and y-axes in figure 1), while P_2 corresponds to the linear polarization fraction referenced along the directions canted 45° and 135° from the horizontal [12]. Figures 2(b) and (c) show that after passing through the lens, the beam becomes linearly polarized with a radial polarization direction. The circular polarization fraction P_3 is exactly zero across the entire cross-section, as required by symmetry. Figure 2(d) shows the total degree of polarization of the beam, P_{tot}, in cross-section, where:

$$P_{\text{tot}} = \sqrt{P_1^2 + P_2^2 + P_3^2}, \tag{1}$$

and increases with radial distance from the principal axis. The induced polarization was confirmed to be perfectly radial by inserting a simulated perfect linear polarizer between the lens and the beam-stop and observing that the transmitted total intensity was constant as the polarizer rotated in a plane perpendicular to the beam axis.

This radial contaminant polarization is potentially problematic for anyone interested in high-accuracy polarimetry, as the collimating lens has changed the polarization of the light to be measured. Such effects are equally if not more problematic for polarization-aided imaging technologies [15, 16]. One solution to reduce, at least in part, the amount of contaminant polarization is to pass the beam through an iris before it reaches the analyzing optics. Since the degree of polarization increases with radial distance from the center of the beam, one could, at the expense of signal strength, tune out the amount of contaminated light present in the beam by selecting the radius of the iris. To this end, we have plotted P_{tot} as a function of distance from the center of the beam cross-section, that is, along the black line in figure 2(d). Figure 3 shows these plots for the AR coated plano-convex lenses oriented with both the planar and curved faces upstream.

Figure 3 indicates that the contaminant polarization increases with distance from the beam center and, for a particular focal length, is larger when the light is incident upon the curved side of the lens compared to the planar side. Both of these results are explained by the fact that the Fresnel-induced polarization increases with increasing angle of incidence upon the lens surface. Thus, we are faced with the following conundrum: while using a lens with a smaller f-number allows us to capture more light, it also introduces more contaminant polarization. It is therefore important to quantify how the Fresnel-induced polarization would affect high-accuracy polarimetry measurements.

Stokes polarization parameters of a beam of light are typically measured by passing it through a retarder followed by a linear polarizer [12]. The angular position of the polarizer is usually fixed, and the retarder rotates in a plane perpendicular to the beam axis. A FFT of the transmitted intensity as a function of the angular coordinate of the fast axis of the retarder allows one to calculate the relative Stokes parameters of the light.

As seen from figure 2, the Fresnel-induced polarization is linear and oriented radially when it strikes the retarder. Thus, the light's linear polarization vector will make an angle with the retarder's fast axis that varies azimuthally within the beam. As a result, the Fresnel-induced polarization altered by the retarder continuously changes from radial linear to circular (ignoring handedness), with an angular periodicity of 90° around the beam cross-section. As the retarder rotates, changing the relative angle between its fast axis and the pass axis of the downstream polarizer, the beam intensity at a fixed

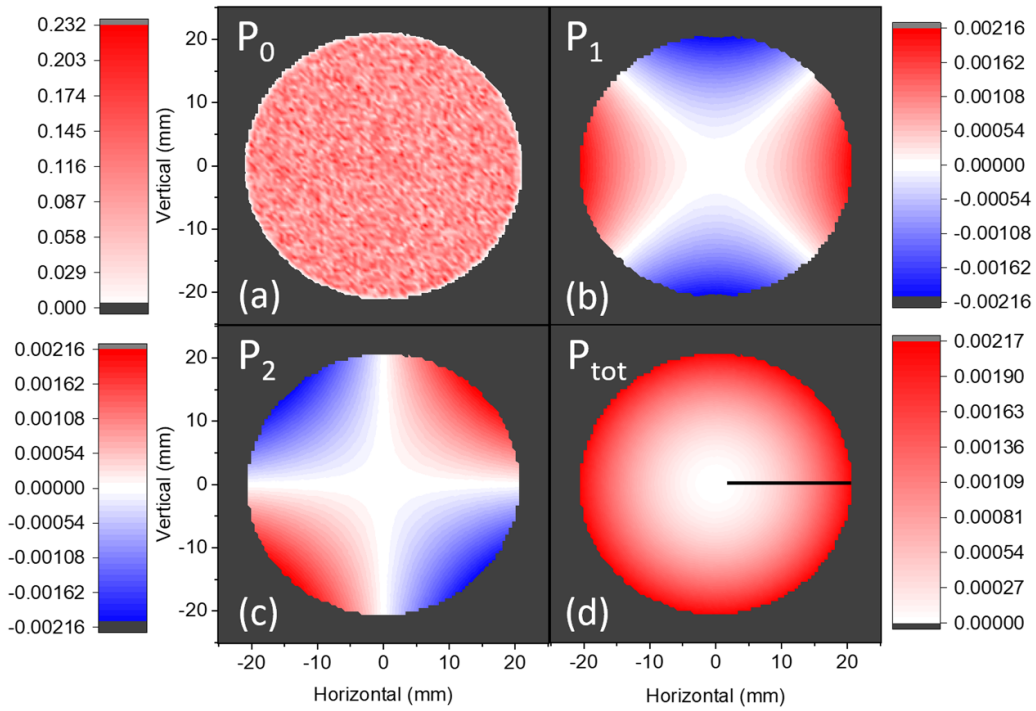

Figure 2. Stokes parameters of the beam in cross-section after passing through the collimating lens. The incident light was initially unpolarized. (a) Beam cross-section of P_0 (intensity), (b) beam cross-section of P_1, (c) beam cross-section of P_2, and (d) beam cross-section of the degree of polarization, P_{tot}. By symmetry, the value of P_3 is identically zero across the entire cross-section and thus is not shown.

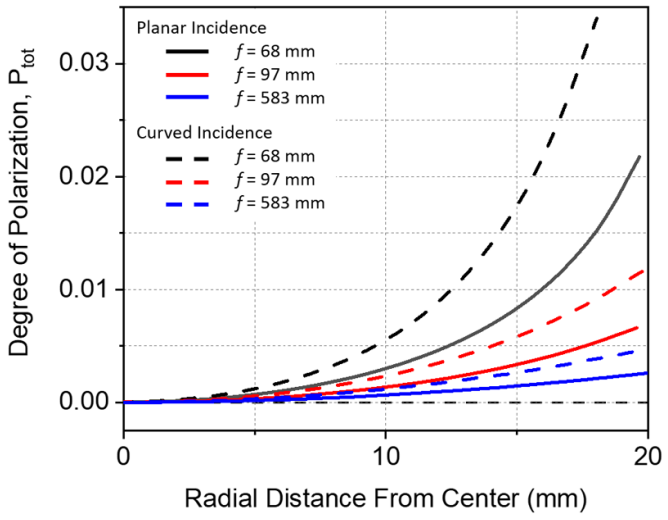

Figure 3. Degree of Fresnel-induced polarization, P_{tot}, as a function of distance from the center of the beam (i.e. along the black line in figure 2(d)) for focal lengths $f = 68$ mm (black), $f = 97$ mm (red), and $f = 583$ mm (blue). The curves for the 583-mm focal length have been multiplied by a factor of 20. The solid lines correspond to the planar side of the lens facing upstream, while the dashed lines are for the curved side facing upstream.

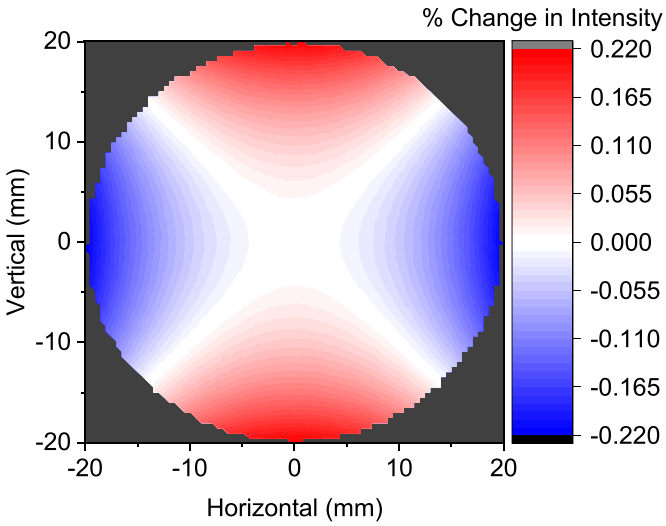

Figure 4. Percentage change in intensity of the beam over its cross-section at the beam-stop when the retarder rotates through 45°.

azimuth will vary downstream of the polarizer, which can, in the case of imperfect analyzing optics, result in a change in the overall transmitted intensity and thus the calculated polarization.

To illustrate this, we first examine, in cross-section, the changes in the beam's intensity after passing through the polarizer as a function of the angular position of the rotating retarder. Again, since the point-source produces unpolarized light, one would expect that in the absence of the Fresnel-induced polarization caused by the lens, the intensity reaching the beam-stop would be constant as the retarder rotates. Figure 4 shows the Fresnel-induced intensity change as the retarder rotates through 45°. The intensity of the beam can change locally by over 0.2%.

These simulations have the advantage that we can analyze the spatial properties of the beam in cross-section. In

FFT polarimetry, however, one measures the integrated beam intensity. When integrating over the entire beam cross-section in figure 4, which was generated using a perfect lens and polarization optics, the net change in intensity of the beam is found to be zero, as required by symmetry. Thus, as long as one considers perfect optical components and a perfectly isotropic point-source, one would not be able to detect the presence of Fresnel-induced polarization by rotating the analyzing retarder, and thus a polarimetric measurement using such components would not deviate from the expected value.

3.3. The effect of less-than-ideal optics

However, the optical components used in real experiments are not perfect. If, for example, the lens deviates from spherical symmetry, the retarder has a fast axis with a varying angular orientation or a non-uniform retardance across the clear aperture, or the polarizer has a less-than-perfectly-defined pass axis, the change-in-intensity map in figure 4 would no longer be symmetric, and an overall change in intensity could be detected as the analyzing retarder rotates. Additionally, an atomic point-source generally emits polarized light of varying intensity across the solid angle subtended by the collection lens. All of these factors can lead to asymmetry in maps like that shown in figure 4, with attendant variations in total integrated intensity as the retarder is rotated.

While there are many factors that may cause the Fresnel-induced FFT polarization result to be non-zero (assuming an isotropic, unpolarized source), we focus on the analyzing retarder. Concurrent work with the AESOP high-accuracy polarimeter shown in figure 1 reveals that the uncertainty in the optical characteristics of the analyzing retarder is one of the largest contributors to overall uncertainty in a polarimetric measurement [7]. Additionally, Trantham *et al* have recently shown that imperfections in the lens can also contribute to errors in polarimetric measurements [9].

For this analysis, we constructed within TracePro® several analyzing retarders that deviate from perfection in different ways. One of the retarders comprised 16 domains of varying retardance with an average and standard deviation (88.95° (1.49°)) comparable to the retarder we use in the AESOP polarimeter. A 2nd device had a fixed retardance but each of its domains had a differently oriented fast axis, with these orientations being distributed with a standard deviation comparable the uncertainty in the orientation of the fast axis used by the AESOP retarder (2°) [17]. A 3rd retarder was designed to simulate a sheet made of long polymer chains sandwiched between glass. Rather than the fast axis position being random across the area of the retarder, it changed continuously, as if the long polymer chains were bending smoothly across the clear aperture. From one edge of the retarder to the other, the angular position of the fast axis could change by up to 90°, with a 5° variation illustrated in figure 5. The fast axis orientation was a function of the horizontal Cartesian coordinate only. The retardance of this retarder was taken to be 90° everywhere.

With these imperfect analyzing retarders in the optical train shown in figure 1, we simulated polarimetry measurements

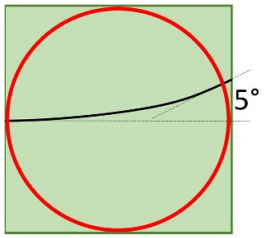

Figure 5. An illustration of the third imperfect analyzing retarder used in the simulations. The fast axis orientation of this retarder continuously changed across its area such that the angle between the fast axis on one side compared to the other was 5°. The angle in the figure is exaggerated.

on isotropically-emitted light produced by a point-source. The focal length of the collimating lens was 155 mm. We calculated the integrated intensity of the beam at the beam-stop (simulating the signal detected by an actual photodetector) for various angular positions of the analyzing retarder. Then, with transmitted total intensity as a function of the retarder angular position, we determined the relative Stokes parameters of the light using the FFT method [12].

When the point-source produced unpolarized light (relative Stokes parameters $P_1 = P_2 = P_3 = 0$), the measured Stokes parameters do not deviate significantly from their expected null values. Even with a retarder with a 90° variation in the fast axis orientation (which is unrealistically bad), rather than the 5° indicated in figure 5, the measured Stokes parameters of the unpolarized light were on the order of 10^{-7}. These results are not a surprise when one considers carefully the data in figures 2(d), 3, and 4. The degree of polarization induced by reflection and refraction is quite small (less than 0.035 even for the most severely curved lens), and the analyzing retarder affects only the polarized component of the light. Thus, when the light is unpolarized, the Fresnel-induced polarization is small enough in magnitude that there is not a significant effect on polarimetric measurements.

Having said this, one rarely makes polarization measurements of unpolarized light. We now consider a highly-polarized atomic fluorescence point source, corresponding to the Ne $3s^3P_2$–$3p^3D_3$ 640-nm transition, that is completely horizontally (x-axis), linearly polarized light ($P_1 = 1$, $P_2 = P_3 = 0$). The intensity of the light emitted by the point-source was still uniform along the y-axis, but decreased in either direction from the point source along the x-axis, in an approximation of the $\sin^2\vartheta$ fluorescence emission distribution associated with fully-horizontally-polarized $p \rightarrow s$ transitions [18]. The intensity of the light as it was incident upon the clear aperture of the lens is shown in figure 6. The coordinate (0, 0) in figure 6 is the center of the lens while the propagation direction of the light is into the plane of the figure. For the simulations, the intensity on the left and ride sides of the beam was 90% of the intensity in the central bright strip in an approximation of the $\sin^2\vartheta$ fluorescence emission distribution.

Again, polarimetry is performed using the FFT method using retarders similar to that shown in figure 5 with progressively larger angular deviations. The measured values of P_1 for these retarders is shown in figure 7. When the angular

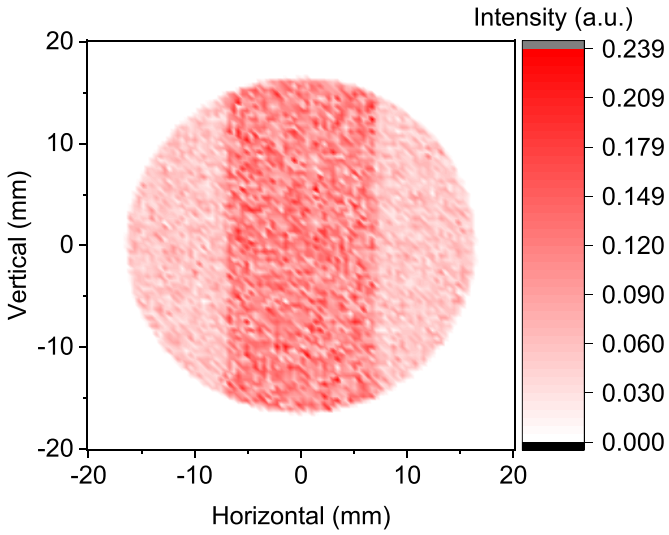

Figure 6. A map of intensity incident upon the collection lens for the simulated, fully linearly-polarized Ne 640-nm $p \rightarrow s$ fluorescence. The difference in intensity between the sides and the middle portions of the beam has been exaggerated for the sake of clarity.

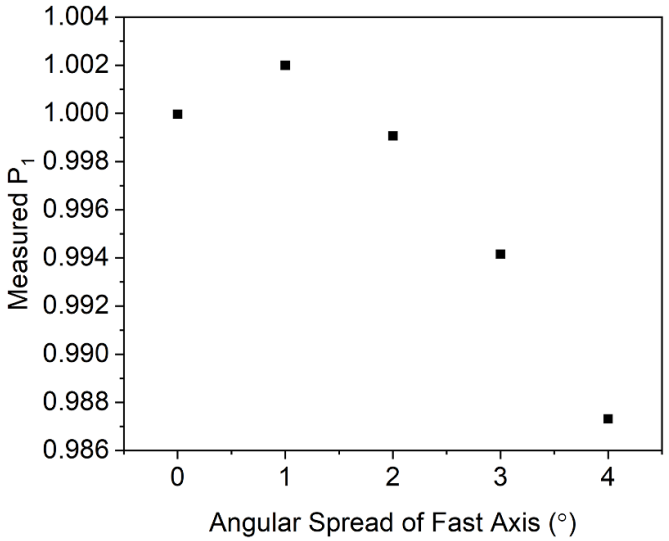

Figure 7. Measured P_1 for the simulated fluorescent light as a function of progressively worse angular spread in the fast axis of the analyzing retarder using a plano-convex lens of focal length 155 mm with its flat surface facing upstream.

spread of the fast axis is 1°, the FFT approach (which cannot account for angular variation of the fast axis) returns an unphysical P_1 of 1.002. By the time we reach a maximum angular deviation in the fast axis of 4°, we find that the difference between the measured value of P_1 and the expected value is greater than 1%—a threshold we deem unacceptable for accuracy requirements at the 0.1% level such as those of the AESOP polarimeter.

The data in figure 7 is for the lens oriented with the planar side upstream. Similar polarimetric simulations for the curved side of the lens facing upstream results in changes of P_1 essentially identical to those shown in figure 7, but varying

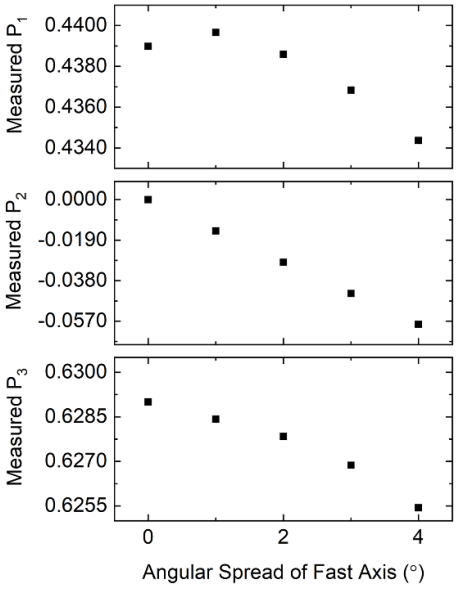

Figure 8. Measured Stokes parameters for the simulated Ar $2p_9$ 811-nm polarimetric transition as a function of progressively worse angular spread in the fast axis of the analyzing retarder using a plano-convex lens of focal length 155 mm with flat surface facing upstream.

from them by about one part in 10^4, easily detectable by the AESOP polarimeter [7].

We now investigate the polarimetry of non-linearly polarized light and find similar errors in the measured Stokes parameters. For this investigation, we modify our source light to simulate another important case related to AESOP involving a different fluorescent wavelength. From [8], we have:

$$P_3 = \gamma\,(1 + \beta P_1)\,P_e \equiv A P_e. \tag{2}$$

At threshold, where this equation holds strictly, for an Ar target and monitoring the 811-nm $2p_9$ polarimetry transition, $A = 0.7317$. Since $\gamma = 2/3$ and $\beta = 2/9$ for Ar, this means that $P_1 = 0.439$ (the value of $P_2 = 0$ at threshold). The Continuous Electron Beam Accelerator Facility (CEBAF) usually runs with a P_e of ∼0.86 [19], so $P_3 = 0.629$. Thus, accounting for the $\sin^2\vartheta$ fluorescence emission by attenuating the right and left sides of the beam by 0.7% (similar to figure 6), we repeat the simulations for a 155-mm focal length collection lens. As before, the angular spread of the fast axis of the analyzing retarder is gradually increased. The results of the simulations are shown in figure 8.

Again, we see that by the time we reach an angular spread of 4° in the fast axis of the analyzing retarder, the error in the measured Stokes parameters becomes unacceptably large—about 1.2% in P_1. We note that P_2, which is supposed to be identically zero, is an easily measurable −5.8%. This is important because P_2 for this transition provides a null test to determine the validity of equation (2) [8]. We see from the results of the simulated fluorescence polarimetry that when the light is not initially unpolarized, the effects of the Fresnel-induced polarization by the lens and the imperfect analyzing optics are much more significant. Once the optics, and in particular the analyzing retarder, begin to deviate from ideal

specifications even slightly, the effect on the measured Stokes parameters can become unacceptably large for high-accuracy polarimetric measurements. It is therefore extremely important to completely characterize the analyzing optics to be used in any high accuracy polarimetry experiment: defects in the optical components will be unique to each component (even if they have the same manufacturer's part number!), and even slight defects can cause measurable deviations from the true polarization.

3.4. Misalignment effects

Finally, we consider the effect of optical misalignment on polarimetric accuracy. Referring to figure 1, the point source is translated along the *y*-axis, though the direction of its emission axis is not changed. We find that for a collimating lens with a focal length of 155 mm, even if the light is unpolarized and the analyzing retarder is perfect, an axial misalignment of 3 mm produces Stokes parameters on the order of one part in 10^5 different from the expected value, which is detectable by the AESOP polarimeter [7]. This can be understood by considering figure 4. When the point source is misaligned with the optical train, the symmetry in the intensity of the light incident upon the analyzing retarder is broken. Therefore, when the retarder rotates during a measurement, the intensity of the radial polarization induced by the collimating lens and parallel to the fast axis of the retarder is not constant. The effect of misalignment becomes more dramatic if the point source produces polarized light and the retarder is not perfect. For example, for the linear horizontally polarized light and the analyzing retarder shown in figure 5 with a focal length of 155 mm, a 3-mm axial misalignment produces error on the order of one part in 10^3, which is readily detectable by the AESOP polarimeter.

4. Conclusions and best practices

Though the issue of lens orientation has been addressed as it relates to spherical aberration, it had not, to our knowledge, been discussed in the literature for photon-counting measurements using dim sources. We thus endeavor to codify best practices in this regard for such experiments. Using the sophisticated ray-tracing software TracePro®, we have systematically addressed the issue of lens orientation and Fresnel reflection- and refraction-induced polarization for a collimating plano-convex lens as it relates to light capture and transmission, polarization-sensitive imaging, and, most importantly, for high-accuracy polarimetry.

From these results, we conclude that for a given focal length, an AR-coated plano-convex lens with the planar side oriented toward the point-source will minimize the amount of light scattered by the lens. Though a lens with small focal length collects more light from the point-source, it also results in more contaminant polarization. We have mapped in cross-section the Fresnel-induced polarization for a beam of light resulting from its passage through the collimating lens. The induced polarization is linear along a radial direction of the beam cross-section. Though the degree of Fresnel-induced polarization is small, it may be of concern to those wishing to do high resolution polarization-sensitive imaging, or those undertaking highly accurate optical polarimetry. In the latter case, we have investigated the effect of the induced polarization on such measurements. Provided that the light is initially unpolarized, the Fresnel-induced polarization has very little effect on the experimentally-determined values of the Stokes parameters. It will be of concern, however, when the analyzing polarization optics are not ideal and the light is initially polarized with an intensity profile that is not isotropic. In this case, the effect may be large enough to lead to significant systematic error in polarimetric measurements. Misalignment of the polarimeter optical train relative to the emission axis of the light source of a few degrees can become important at the 10^{-3} level for Stokes parameter measurements.

The general rule that the collection lens should have its surface with the largest radius of curvature facing upstream holds for issues related to maximal transmission and polarimetric accuracy, as well as for issues related to image formation. Finally, we recommend that for highly accurate polarimetry, comprehensive ray-tracing software be used to construct detailed numerical models of the experimental apparatus being used in order to characterize potential sources of uncertainty.

Data availability statement

The data that support the findings of this study are available upon reasonable request from the authors.

Acknowledgments

The use of TracePro® was made possible by an academic license supplied by Lambda Research Corporation. The authors thank Lambda Research Corporation for its support.

Conflict of interest

The authors declare no conflicts of interest.

Funding

Financial support for this work was provided by the National Science Foundation (NSF) under Grant No. PHYS-1632778.

ORCID iDs

K D Foreman https://orcid.org/0000-0001-9353-552X
T J Gay https://orcid.org/0000-0001-9208-1570

References

[1] Hough J 2006 Polarimetry: a powerful diagnostic tool in astronomy *Astron. Geophys.* **47** 3.31–3.35
[2] Stam D M, Hovenier J W and Waters L B F M 2004 Using polarimetry to detect and characterize Jupiter-like extrasolar planets *Astron. Astrophys.* **428** 663–72
[3] Qiu Z Q and Bader S D 2000 Surface magneto-optic Kerr effect *Rev. Sci. Instrum.* **71** 1243–55

[4] Ding H F, Pütter S, Oepen H P and Kirschner J 2001 Spin-reorientation transition in thin films studied by the component-resolved Kerr effect *Phys. Rev.* B **63** 134425
[5] Commins E D and Bucksbaum P H 1980 The parity non-conserving electron-nucleon interaction *Annu. Rev. Nucl. Part. Sci.* **30** 1–52
[6] Taylor J D, Baird P E G, Hunt R G, Macpherson M J D, Nowicki G, Sandars P G H and Stacey D N 1987 Measurement of parity non-conserving optical rotation in the 648 nm transition in atomic bismuth *J. Phys.* B **20** 5423–42
[7] Foreman K and Gay T J 2018 Accurate electron spin optical polarimetry (AESOP) *Bull. Am. Phys. Soc.* **63** 56 (Available at: https://meetings.aps.org/Meeting/DAMOP18/Session/E01.55)
[8] Gay T J, Furst J E, Trantham K W and Wijayaratna W M K P 1996 Optical electron polarimetry with heavy noble gases *Phys. Rev.* A **53** 1623–9
[9] Trantham K W, Foreman K D and Gay T J 2020 Demonstration of vacuum strain effects on a light-collection lens used in optical polarimetry *Appl. Opt.* **59** 2715–24
[10] Gay T J 2009 Physics and technology of polarized electron scattering from atoms and molecules *Adv. At. Mol. Opt. Phys.* **57** 157–247 (Available at: www.sciencedirect.com/science/article/pii/S1049250X09570048)
[11] Furst J E, Gay T J, Wijayaratna W M K P, Bartschat K, Geesman H, Khakoo M A and Madison D H 1992 An attempt to observe Mott scattering optically *J. Phys.* B **25** 1089
[12] Berry H G, Gabrielse G and Livingston A E 1977 Measurement of the Stokes parameters of light *Appl. Opt.* **16** 3200–5
[13] Moore J H, David C C and Coplan M A 2009 *Building Scientific Apparatus* 4th edn (Cambridge: Cambridge University Press) ch 4
[14] Bennett C A 2008 *Principles of Physical Optics* (New York: Wiley) pp 69–92
[15] Oldenbourg J and Mei G 1995 New polarized light microscope with precision universal compensator *J. Microsc.* **180** 140–7
[16] Juang C-B, Finzi L and Bustamante C J 1988 Design and application of a computer-controlled confocal scanning differential polarization microscope *Rev. Sci. Instrum.* **59** 2399–408
[17] Wolenski C 2020 *Private Communication (Meadowlark Optics Inc.)*
[18] Feofilov P P 1961 *The Physical Basis of Polarized Emission* (New York: Consultant's Bureau) p 23
[19] Grames J M *et al* 2020 A high precision 5 MeV Mott polarimeter *Phys. Rev.* C **102** 015501